Journal of Proteomics 148 (2016) 194–201

Contents lists available at ScienceDirect

Journal of Proteomics

journal homepage: www.elsevier.com/locate/jprot

Phosphoproteomic analysis of the posterior silk gland of *Bombyx mori* provides novel insight into phosphorylation regulating the silk production

Jia Song, Jiaqian Che, Zhengying You, Lupeng Ye, Jisheng Li, Yuyu Zhang, Qiujie Qian, Boxiong Zhong *

College of Animal Sciences, Zhejiang University, 866 Yuhangtang Road, Hangzhou 310058, PR China

ARTICLE INFO

Article history:
Received 14 May 2016
Received in revised form 3 August 2016
Accepted 9 August 2016
Available online 13 August 2016

Keywords:
Bioinformatics
Bombyx mori
Posterior silk gland
Phosphoproteomics
Silk

ABSTRACT

To understand phosphorylation event regulating silk synthesis in the posterior silk gland of *Bombyx mori*, phosphoproteome was profiled in a pair of near-isogenic lines, a normally cocooning strain (IC) and a nakedly pupated strain (IN) that the silk production is much lower than IC. In the posterior silk gland of the IC and IN, 714 and 658 phosphosites resided on 554 and 507 phosphopeptides from 431 and 383 phosphoproteins, were identified, respectively. Of all the phosphosites, the single phosphosite was the dominate phosphorylation form, comprising > 60% of all the phosphosites in two phenotypic of silk production. All these phosphosites were classified as acidophilic and proline-directed kinase classes, and three motifs were uniquely identified in the IC. The motif S-P-P might be important for regulating phosphorylation network of silk protein synthesis. The dynamically phosphorylated proteins participated in ribosome, protein transport and energy metabolism suggest that phosphorylation may play key roles in regulating silk protein synthesis and secretion. Furthermore, fibroin heavy chain, an important component of silk protein, was specifically phosphorylated in the IC strain, suggesting its role to ensure the normal formation of silk structure and silk secretion. The data gain new understanding of the regulatory processes of silk protein synthesis and offer as starting point for further research on the silk production at phosphoproteome level.

Significance of this study: Despite the knowledge on regulation of silk protein synthesis in the posterior silk gland has gained at the gene or protein levels, how phosphorylation event influences the silk yield is largely unknown. To this end, we constructed a pair of silkworm near-isogenic lines that showed different cocooning phenotypes, and the phosphoproteome of the posterior silk gland of two isolines was compared. Here, we reported the first phosphoproteome data on the silkworm and found several key pathways related protein synthesis are regulated by phosphorylation, thereby influencing the silk production. The data provide valuable resources for further functional assay of targeted protein phosphorylation that regulates the silk synthesis in silkworm.

1. Introduction

Protein activity can be regulated at three main levels: transcriptional, translational controls and post-translational modifications (PTMs). Compared with transcriptional and translational controls, PTM of proteins can efficiently drive adaptive cellular responses by adding or removing functional groups from protein residues [1]. Among the variety of PTMs, phosphorylation has been extensively studied in prokaryotes and eukaryotes [2,3]. Recently, with the aid of developments in electric ion source and high-throughput technology, mass spectrometry (MS) has become a viable alternative to more traditional methods of phosphorylation analysis [4,5].

The domesticated silkworm, *Bombyx mori*, has long been used as a model system in basic research [6]. Its silk gland, a highly efficient protein synthesis machine, is a suitable model for probing the mechanism of gene specific expression and regulation. Therefore, posterior silk gland (PSG), the most important and largest part, is responsible for synthesizing the silk core protein, fibroin, which is a complex of heavy chain (Fib-H), light chain (Fib-L) and glycoprotein P25. In silkworm genetic resource database, several cocoon-mutant strains in which the synthesis of silk proteins blocked are selected for studying the compounding mechanism of synthesizing silk proteins. Among them, a naked-type strain called "Nd" is frequently studied, and the mutated gene is located on chromosome 25 at site 0.0 [7].

Near-isogenic lines, also called isolines, are characterized by two or more strains with fully identical traits and genetic backgrounds except for one pair of alleles. Because there are only one or two differences, isolines provide an ideal system for researching genetic function [8]. The similarities and specific differences between an isoline and its recurrent parent can facilitate analysis of the influence of a desired gene on character and physiology.

* Corresponding author.
E-mail address: bxzhong@zju.edu.cn (B. Zhong).

http://dx.doi.org/10.1016/j.jprot.2016.08.007
1874-3919/

In recent years, with the increasing development of proteomic technologies, the biological processes regulating silk yield in silkworms have been investigated. It is reported that the up-regulation of ribosomal proteins, protein degradation and energy metabolism is important for fibroin synthesis and highly efficient protein synthesis system [9,10]. Several synthesis-related proteins from silkworms with adequate nutrient absorption are up-regulated, thus guaranteeing normal function of silk gland cells and enhancing protein synthesis [11]. However, knowledge regarding how phosphorylation events regulating the silk production in PSG is still lacking. Hence, the aim of this work is investigating the regulation of silk production by comparing the phosphopropteome of a pair of isolines. These results are expected to offer better comprehension and utilization of the silk gland in future applications.

2. Materials and methods

2.1. Construction of a pair of near isogenic lines

A pair of near-isogenic lines, bred by our lab, named IC with normally pupated and IN with naked pupated was utilized as the experimental materials. To breed them, two silkworm strains, the naked pupa (Nd) with normal markings and the naturally pupated strain whose larvae have striped markings (p^s), were selected and multiply hybridized (Fig. S1). The Nd and p^s gene were dominant on pupation form and body color, respectively. First, the Nd strain and the p^s strain were hybridized to produce F_1 generation, characterized by naked pupation at the pupal stage. Then, the F_1 generation was backcrossed with the p^s strain, and their offspring, namely BC_1 generation, represented two phenotypes, including pupation without cocoons and with normal cocoons. Among them, the normally pupated individuals were discarded and the naked pupated individuals were kept. This backcross method was repeated until the BC_{17} generation to ensure that only the *Nd* gene was transferred into the p^s strain. Then, the nakedly pupated larvae of BC_{18} generation were inbred with compatriots from the same brood. The offspring presented clear segregation of character, including nakedly pupated individuals and normally cocooned individuals (the phenotypic ratio was 3:1). To obtain homozygotes, the nakedly pupated individuals were crossed with their siblings with identical phenotype from the same brood. After the BC_{20} generation was generated, we merely reserved the broods with single phenotype of naked pupa. Then some of the nakedly pupated individuals from one brood were chosen to cross with the p^s strain, and the remaining individuals were crossed with their compatriots from the same brood to produce the BC_{21} generation. When the offspring from more than eight broods obtained by backcrossing with the p^s strain didn't represent character segregation, the Nd gene of this brood was homozygous ($P > 0.996$). Here, we named this family as IN, and the backcross parent was named IC. The key difference between IC and IN was whether the larvae spun and cocooned at the pupal stage.

2.2. Organ isolation and protein preparation

The experiment setups were basically followed previous description with some modifications [3]. The PSGs from 10 silkworms of each strain were sampled on day 3 of fifth instar, a key time point for massive silk protein synthesis. Samples were dounce-homogenized in lysis buffer (8 M urea, 40 mM Tris-base, 65 m Mdithiothreitol (DTT), 4% 3-[(3-cholamidopropyl) dimethylammonio]-1-propanesulfonate (CHAPS), each tablet complete mini protease inhibitor mixture (Roche, Basel, Switzerland) per 10 mL and each tablet phosphatase inhibitor cocktail (Roche, Basel, Switzerland) per 10 mL). The mixture was sonicated for further lysing, and centrifuged at 15,000 g for 45 min. DTT (1 M, 2 μL) was added into the quantified supernatant (500 μg), and the sample was incubated at 37 °C for 2.5 h. Then iodoacetamide (1 M, 10 μL) was added to incubate for 40 min at room temperature in the dark. The lysate was precipitated overnight by 100% acetone and then diluted by 100 mM ammonium bicarbonate (PH 8.5). Sequencing grade trypsin (Promega, Madison, MI) was used at a ratio of 1/50 (trypsin/protein) and enzymolysed overnight. TFA was added to terminate the digestion. The insoluble materials were removed by centrifuging and then desalted by C18 SepPak cartridges (Waters, Milford, MA). The obtained elutes were lyophilized and stored for the following experiment. During the entire process, protein concentration was measured by using a Bio-Rad Protein Assay Kit (Bio-Rad, Hercules, CA).

2.3. Phosphopeptide enrichment with titanium dioxide tips

Phosphopeptide enrichment procedures were performed on a previous method [12]. Briefly, TiO_2 beads were equilibrated by addition of 100 μL loading buffer (saturated glutamic acid, 65% ACN, 2% TFA), and the prepared peptide mixture was loaded onto the TiO_2 column. The mixture was incubated with end-over-end rotation for 60 min at room temperature. After incubation, the slurry was centrifuged and washed with 100 μL washing buffer 1 (65% ACN, 0.5%TFA), and 100 μL washing buffer 2 (65% ACN, 0.1% TFA) and centrifuged again. Then, the phosphopeptides were eluted with 100 μL elution buffer (300 mM ammonium hydroxide, 50% ACN). The flow through was then collected, dried and prepared for further analysis.

2.4. Nano LC-MS/MS analysis

The nano LC-MS/MS was carried out as previously described [13]. All of the digested phosphopeptide were subjected to LC-LTQ-Orbitrap-MS (Thermo Fisher Scientific, San Jose, CA) in two replicates in each sample. The mixture was analyzed by nano-flow C18 reverse-phase liquid chromatography using a 15 cm fused silica monolithic column (0.075 mm inner diameter) (Column Technology, Fremont, CA). The peptide mixtures were separated using a separating gradient of 2%–35% solvent B (0.1% formic acid in ACN solution) over 120 min at a flow rate of 200 nL/min. The peptide mass spectrum was obtained in positive ion mode using data-dependent automatic switching between MS and MS/MS acquisition modes. The ten most intense ions were selected for MS/MS analysis. Fourier transformed full scan mass spectra were acquired in the range of m/z of 400–2000. The enabling dynamic exclusion and collision energy were set to 90 s (repeat count 2) and 35%, respectively.

2.5. Peptide identification, database search and data filtering

MS/MS spectra were collected for searching by using the target-decoy database searching strategy of the Sequest algorithm [14] against the Silkworm Knowledgebase (SilkDB) (http://www.silkdb.org/silkdb/doc/download.html) and the National Center for Biotechnology Information (NCBI) (http://www.ncbi.nlm.nih.gov/). The parameters included tryptic specificity, a mass tolerance of 10 ppm, up to 2 miscleavage sites, and a unique static modification of 57.0215 Da (carboxyamidomethylation) on cysteine. The results were analyzed as described [15,16], which used decoy matches as a guide. The filtering criteria, like Delta Cn, were applied to achieve a 1% false discovery rate. To localize phosphorylation sites, manual interpretation of the MS/MS ion spectra was utilized. The primary criteria of manual interpretation on MS/MS spectra was that the matched number of the b or y ions of continuous amino acids was designed as over four [12]. And most high abundant peaks in MS/MS spectra could match to b or y ions and the neutral loss ions. To count and classify the significantly altered phosphoproteins, the fold change of the identified phosphopeptide quantities in the IN strain against the IC strain was calculated. Phosphoproteins with fold changes ≥ 1.5 or ≤0.67 were considered to be increased or decreased.

2.6. Motif analysis

Phosphopeptide sequences were submitted to the Motif-X algorithm (http://motif-x.med.harvard.edu/) for discovering phosphorylation motifs [17]. The background was the uploaded *B. mori* proteome (a < 10 m database that was randomly generated from *B. mori* proteome). The sequence was centered on each phosphorylation site and extended to 13 amino acids (±6 residues). Because the Motif-X algorithm excluded the N or C termini, these sites could not be extended. The number of motif occurrences was 20, and the significance threshold was set to $P < 10^{-6}$. The extracted motifs were used to determine the kinase classes, including acidic, proline-directed, basic, tyrosine and others, based on substrate sequence specificity [18]. The simplified categorization is useful because kinase specificity is often defined by amino acid motifs that surrounded serine (Ser), threonine (Thr) and tyrosine (Tyr) residues of the substrate proteins.

2.7. Bioinformatics analysis

Identified differentially changed phosphoproteins were classified according to cellular component, molecular function, and biological process by retrieving the Gene Ontology (GO) annotation database, an integrated web-based GO analysis toolkit for the agricultural community, agriGO (http://bioinfo.cau.edu.cn/agriGO/). The biological pathways were mapped using the online Kyoto Encyclopedia of Genes and Genomes (KEGG) (http://www.genome.jp/kegg/) to obtain the corresponding KEGG pathways, and each pathway mapped by over 2 proteins in either strain was chosen for functional analysis.

3. Results and discussion

3.1. Biological characteristics and phosphoproteomic profiling

To gain an insight into the molecular details accounting for significantly low silk yield, a pair of isolines, IC and IN, was constructed to probe the effects of transferring the *Nd* gene. For the IN, although the length of anterior and middle silk gland were almost similar, the PSG was significantly shorter than that in the IC strain (Fig. 1A). Moreover, in the pupal stage, we could visually observe that the larvae of the IN strain were nakedly pupated and had not spun cocoons. In contrast, the IC strain was normally cocooned (Fig. 1A). By comparing the phenotypes of the IC and IN, the differences in silk production were significantly different. Subsequently, the probable causes leading to lower silk production on IN was investigated by phosphoproteomic techniques.

In all, 884 and 782 non-redundant phosphopeptides from 520 phosphoproteins and 445 phosphoproteins were identified in the IC and IN strain, respectively (Supplemental Table 1). 1580 phosphopeptides from 345 phosphoproteins and 2058 phosphopeptides from 460 phosphoproteins in each of two samples were identified in the IC strain (Supplemental Table 1). In the IN strain, 1224 phosphopeptides from 338 phosphoproteins and 1639 phosphopeptides from 360 phosphoproteins were identified in each of two samples (Supplemental Table 1). Applying filtering criteria, 554 and 507 non-redundant phosphopeptides derived from 431 and 383 phosphoproteins, were identified in the IC and IN strain, respectively (Supplemental Table 2). In total, 288 phosphoproteins were shared in the IC and IN strains. The number of up-regulated and down-regulated phosphoproteins was respectively 59 and 94, between the two strains. The numbers of specific phosphoproteins of the

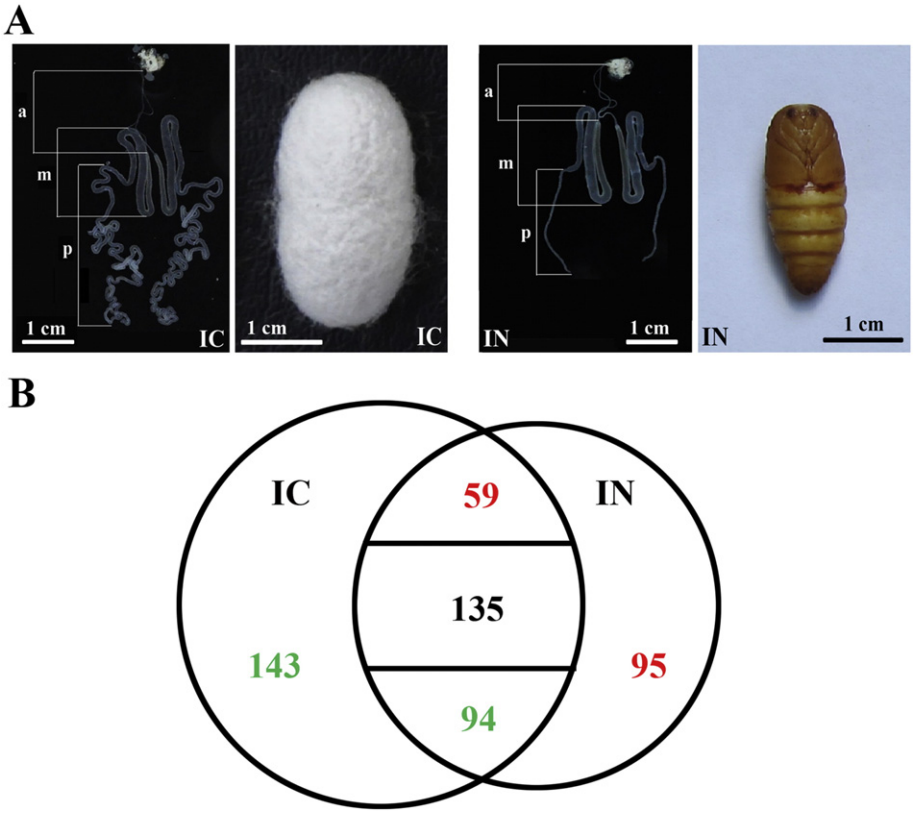

Fig. 1. Phenotypic characteristics and identified phosphoproteins in the IC and IN strains. The length of the silk gland and phenotype in the pupal stage of the IC strain was compared with that in the IN strain (A). The silk gland contained anterior silk gland (a), middle silk gland (m), and posterior silk gland (p) (the region marked by the white lines). The number of phosphoproteins counted in the IC and IN strains (B), the shared number of phosphoproteins is 288 (59 to up-regulated, 94 to down-regulated and 135 to none significantly different), and the specifically identified number of proteins from the IC and IN is 143 and 95, respectively. 154 (59 to common phosphoproteins and 95 to specific phosphoproteins) and 237 (94 to common phosphoproteins and 143 to specific phosphoproteins) mean up- and down-regulated phosphoproteins were identified with the IN was compared to the IC strain.

IC and IN strain were 143 and 95, respectively (Supplemental Table 2 and Fig. 1B). For both the IC and IN, the most phosphorylated protein was elongation factor 1-beta', which 429 and 349 phosphopeptide were identified in each of them. In the IC and IN strains, 19 and 16 phosphoproteins were phosphorylated >20 peptides. Most of them were relevant to protein synthesis, such as ribosomal protein P2 and L22. Moreover, 86.3% and 84.9% phosphopeptides was phosphorylated <10 peptides in the IC and IN strains.

3.2. Phosphorylation sites and motif analysis

A total of 714 and 658 phosphosites were localized in the IC and IN strains, respectively (Supplemental Table 2). The different number of phosphosites in each strain suggest that phosphorylation might play a key role in silk protein process. Multiple phosphorylation events may take place within a short amino acid sequence and may also occur within the same tryptic peptide. Therefore, the distribution of the phosphorylated sites was counted according to the identified data. For each protein, the numbers of the phosphorylated sites on only one residue were 273 (63.3%) and 238 (62.1%) in the IC and IN, respectively (Fig. 2A and Supplemental Table 2). The protein with the largest phosphosite number, 9 phosphosites, was ATP-binding cassette subfamily F member 1 in the IC, and titin protein was phosphorylated on up to 13 residues in the IN. Most of peptide contained only 1 phosphosite, corresponding 73% in both IC and IN; moreover, the highest phosphosite number was 4 in one peptide in both IC and IN (Fig. 2B). These results indicate that most proteins and peptides mainly phosphorylated on single site in *B. mori*. By examining the frequency of all the identified phosphosites, the most observed phosphorylated amino acid was Ser (85.2%), followed by Thr (13.0%) and Tyr (1.9%) in the IC strain. These were essentially consistent with those acquired for the IN strain (Fig. 2C). The majority of the identified phosphosites were phosphorylated at Ser residues, reflecting a strong preference for Ser phosphorylation in both the IC and IN strains.

From extracted motifs of the phosphorylation data set, only acidic and proline-directed kinase classes, which a similar proportion between the two strains, were discovered (Fig. 3A). The results indicate that these two kinase classes implicated in most of the phosphorylation events in the PSG to sustain the normal biological processes. In total, 8 motifs, 6 in acidic class (Fig. 3B) and 2 in proline-directed class (Fig. 3C), were found. Of these, 5 motifs (4 to acidic and 1 to proline-directed) were common in the two strains, and the 3 other motifs were IC-specific (Supplemental Table 3). Almost all the acidic kinase classes were recognized by the protein kinase CK2 whose substrate specificity was best described as S/T-E/D-x-D/E [19,20]. So far, over 300 substrates of the CK2 kinase have been found, and most of them play a vital role in various biological processes. Among the known substrates, over 40 substrates are ribonucleoproteins, at least 60 and 20 ones are transcription and translation factors, respectively, and more than 80 substrates function in cell signaling [21]. These data imply that the process of protein synthesis is highly regulated by phosphorylation in the IC and IN. For proline-directed class, only the protein kinase of motif S-P was recognized as mitogen-activated protein kinase (MAPK) [22]. For 20 phosphoproteins having motif S-P-P, some phosphoproteins participating in genetic material

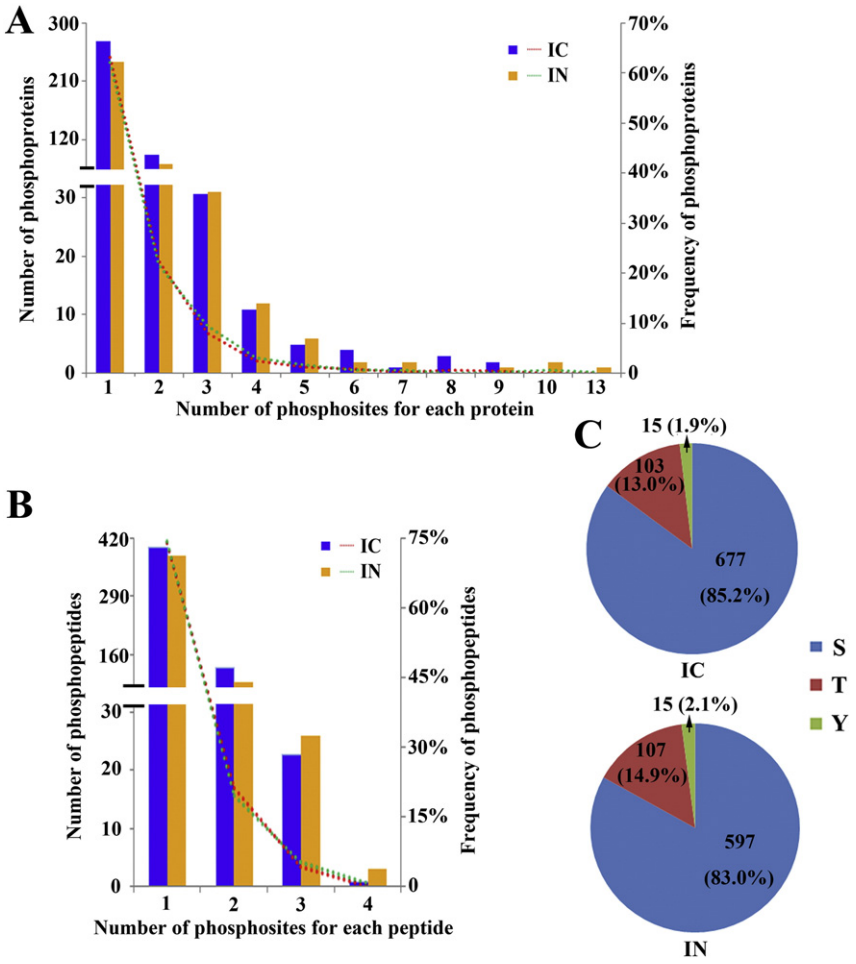

Fig. 2. Overview of the phosphorylation sites in the PSG of silkworm. Bar graphs show the number of phosphosites for each protein (A) and each peptide (B) detected in the distinct strains. The lines represent the corresponding percent. Pie chart shows the distribution of the phosphorylated amino acids in the IC strain (upper) and the IN strain (lower) (C).

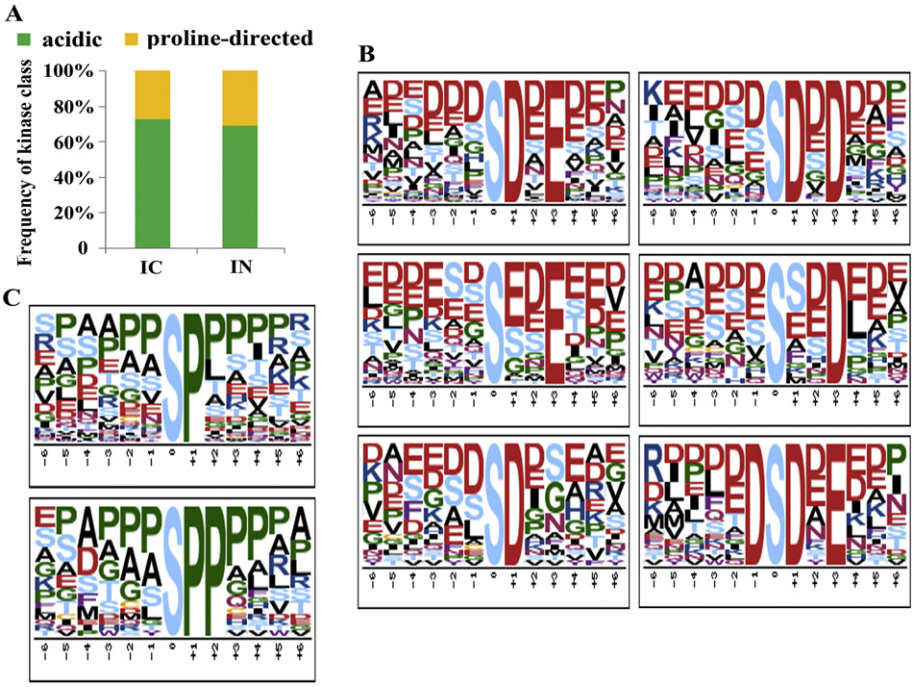

Fig. 3. Characteristics of the motifs identified in *Bombyx mori*. The frequencies of each identified kinase class are counted in the IC and IN (A). Logo-like representations of the phosphorylation motifs were identified by the Motif-X algorithm. Two kinase classes, acidic (B) and proline-directed (C), are enumerated individually. The last two on right line (B) and the lower motif (C) are the IC-specific motifs. The remaining five motifs are shared by the IC and IN strains.

synthesis processes, such as zinc finger protein, polyadenylate binding protein 2. Hence, the kinase recognized motif S-P-P is important to normal synthesis and secretion of silk protein.

Compared our data with those of *Drosophila melanogaster* embryos [3] and *Apis mellifera ligustica* hypopharyngeal gland [23], the only distinction was multiply phosphopeptides possessed higher proportion on fly, however, most proteins preferred single phosphorylation in both silkworm and honeybee. Ser phosphorylation occupied the largest proportion, and acidic and proline-directed motifs were the first two most abundant classes on all the three species. In all, for the silkworm, most proteins were phosphorylated on a single site, suggesting that a single site phosphorylation regulates the majority of the functions of a protein in most cases. That Ser phosphorylation occupied the largest proportion was also in accordance with the existing theory that protein phosphorylation mainly occurs at Ser in eukaryotic cells [24]. And phosphorylation events are mainly accomplished by acidic and proline-directed kinase classes in the PSG of *B. mori*.

3.3. Differentially expressed phosphoprotein analysis

Comparing IN (total 383 phosphoproteins) with IC (total 431 phosphoproteins), 237 phosphoproteins, 143 specific phosphoproteins and 94 common phosphoproteins, showed decreased their expression. Whereas 154 phosphoproteins (95 to specific phosphoproteins and 59 to common phosphoproteins) showed increased expression (Supplemental Table 4 and Fig. 1B). Among the down-regulated phosphoproteins, several proteins involved in genetic material synthesis and secretion were found, such as regulatory factors and secretion-related proteins. Protein translation proceeds in four phases: activation, initiation, elongation, and termination. During the entire process, regulatory factors play important roles. Eukaryotic translation initiation factor 5 (eIF5) is involved in forming a multifactor translation-initiation complex [25]. Once phosphorylation is reduced, the complex formation might be disrupted, thereby influencing translation initiation. As a member of the heterometric βγδ complex, elongation factor 1 delta (EF-1δ) is phosphorylated and subsequently recycles inactive EF-1α GDP to the active GTP-bound form and transfers aminoacyl-tRNAs to the ribosome [26]. In our study, undetected phosphorylation suggests that the protein elongation process is blocked. Calnexin, normally phosphorylated on the cytosolic domain, participates in ER quality control and ensures the secretion of correctly folded proteins and combines with the ribosome and providing favorable conditions for the translation process [27,28]. Here, unphosphorylation suggests that proteins are accumulating, and de novo protein synthesis is impaired in the cells. In cells, it is only when proteins are trafficked to their final destination and assembled into structural and functional complexes that they can play their roles [29]. Therefore, correct protein trafficking and secretion is important. Consequently, the translation process was hindered and generated low protein yields, and thus blocking protein secretion in the IN strain. The down-regulated ribosomal proteins are likely to contribute to decreased proteins synthesis at the translation level has been verified [10]. In the meantime, previous research on in vitro phosphorylation has shown that changes of phosphorylated ribosomal proteins alter the substrate binding sites or the conformation in the ribosome, which leads to a 50% loss of activity in protein synthesis [30,31]. Therefore, the most phosphorylated ribosomal proteins decreased their abundance level might also be responsible for the reduced protein synthesis observed in the IN strain. Acidic ribosomal protein P1 and P2, members of the key protein synthesis organelle that make up the eukaryotic ribosomal stalk. Their phosphorylated forms are implicated in modulating ribosomal function [32]. In the IN strain, the reduced level of these two proteins may led to decreased partial activity and further decreased ribosomal productivity. The phosphorylated ribosomal protein S2 (Rps2) participates in aminoacyl-transfer RNA binding to the ribosome [33]. Low Rps2 phosphorylation may suppress elongation process, thus preventing normal protein synthesis in the IN strain. Some phosphoproteins, such as programmed cell death protein 4-like (PDCD4), involved in the regulation of cell development and apoptosis, showed down-regulated phosphorylation in the IN strain. PDCD4 is associated with transduction of anti-apoptotic signaling by phosphorylated by Akt kinase [34,35]. In the nakedly pupated strain, low level of phosphorylated PDCD4 may accelerate the apoptosis of PSG. In addition, phosphoproteins related to ATP metabolism were specifically expressed in the IC, namely H + transporting ATP synthase beta subunit isoforms 1

and 2. Phosphorylation of ATP synthase-β lowers ATP synthase activity and depresses energy synthesis [36]. Because of the negative phosphorylation, energy production was enhanced in the naked strain, which was consistent with previous results indicating that the strain with low silk yield demand intensive energy metabolism [10]. Notablely, higher energy consumption did not cause a positive productivity change. Comparing with our results and previous proteome data [9, 10], the enhanced energy consumption might be used for ontogenetic processes rather than the synthesis of silk protein. Additionally, of the three main silk components, only phosphorylated fibroin heavy chain (Fib-H) was found to specifically exist in the IC strain. Previous research has shown that the phosphorylation of Fib-H drives its function. Phosphorylation of Fib-H causes a conformational change with functional consequences as well as possibly binding between silk proteins [37]. The reason for the dephosphorylation of Fib-H might be the distinct *Fib-H* sequence of the Nd strain. Compared with the normal strain, partial bases change generates a distinguishing protein structure and thus preventing phosphate group combination [7,38]. Therefore, in the IN strain, unphosphorylated of Fib-H might inhibit the formation of the silk structure and affect silk protein secretion to consequently cause the nakedly pupated phenotype. At the translational level, the expression of Fib-H was not altered, and it has been confirmed that its quantity does not contribute to the difference in cocoon weight [10]. Hence, phosphorylation may be an important factor that influences silk synthesis by varying the protein structure.

Among the up-regulated phosphoproteins, some molecular chaperones were identified, such as 90-kDa heat shock protein (HSP90) and 97 kDa heat shock protein. HSPs can assist in the formation of mature proteins and participate in degrading misfolded proteins [39,40]. As mentioned above, large quantities of non-phosphorylated Fib-H with an abnormal conformation must be eliminated with the aid of abundant HSPs. The phosphorylated HSP90 can participate in the regulation of the G_2/M checkpoint, thus mediating the cell cycle [41]. In the IN strain, over-phosphorylated HSP90 might generate a late nuclear division, supporting the existing conclusion that the aberrant nuclear division of the PSG cell generates a shorter PSG [42]. Several phosphoproteins associated with transport showed increased expression level. Among these proteins, transport protein SEC31 (Sec31) is a typical coat protein II, and its phosphorylation appears to reduce the association with Sec23, thereby limiting the budding of vesicles from the ER membranes and regulating ER-to-Golgi trafficking [43]. Hence, in the IN strain, the phosphorylation of Sec31 may depress vesicle transport and impair proper protein function.

3.4. Bioinformatics analysis of the differentially expressed phosphoproteins

For up-regulated phosphoproteins, there were 13 items were annotated, including 6 to cell component, 2 to molecular function, 5 to biological progress; for down-regulated phosphoproteins, total 31 items were annotated (Fig. 4). Specifically, in the cell component, proteins with decreased phosphorylation were involved in 12 items, and the number of specific items was 8 terms. Thereinto, macromolecular complexes are an essential aspect in cellular processes, including gene expression, cell cycle regulation, cell signaling and metabolism. Thus, the number of bioactive complexes is higher in the IC to ensure normal physiological function, such as sufficient active ribosomes ensured

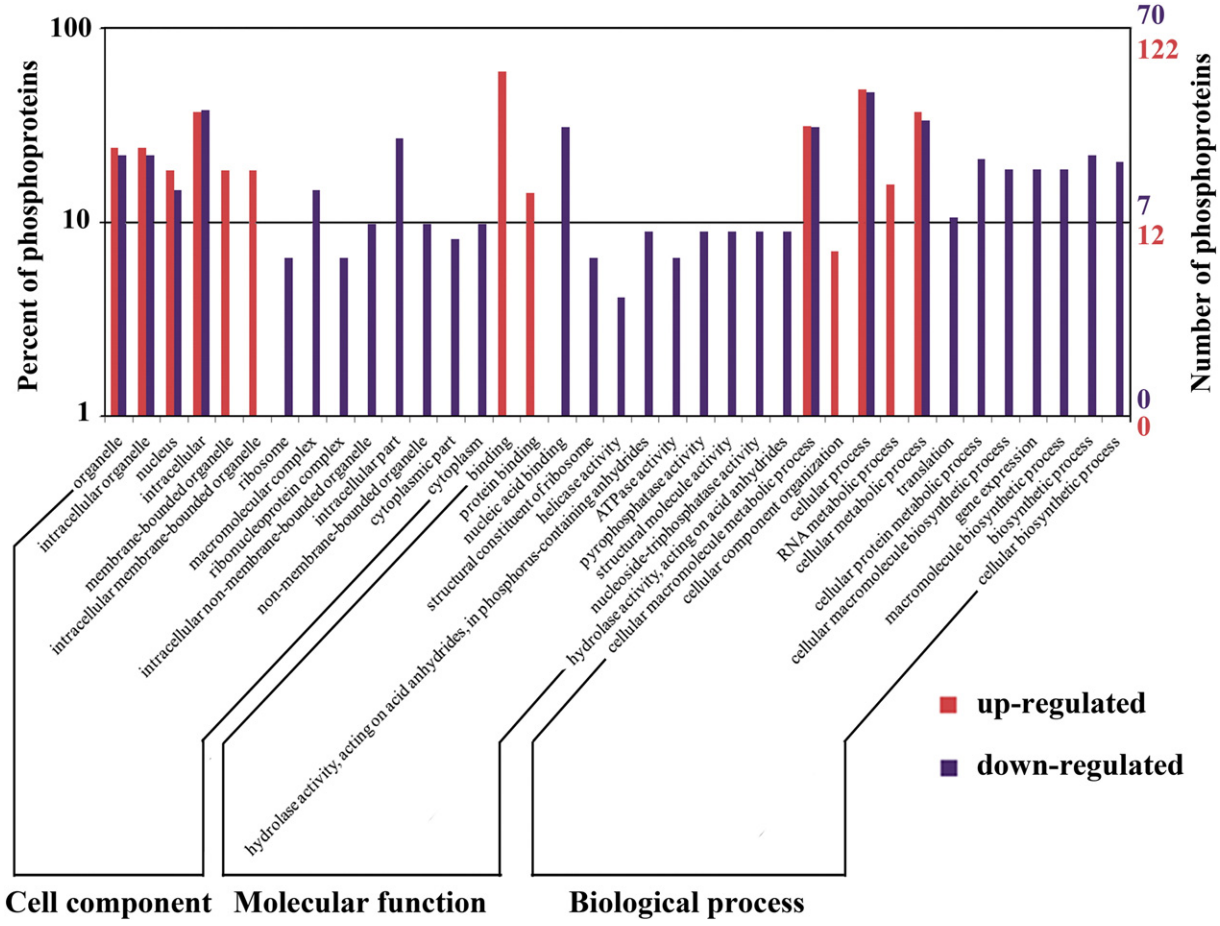

Fig. 4. GO categories of the differentially phosphorylated proteins. The number of phosphoproteins mapping to the GO terms is shown in the right panel. The left panel represents the proportion of phosphoproteins mapping to the GO terms. The light red bar represents the up-regulated phosphoproteins, and the purple bar represents the down-regulated phosphoproteins.

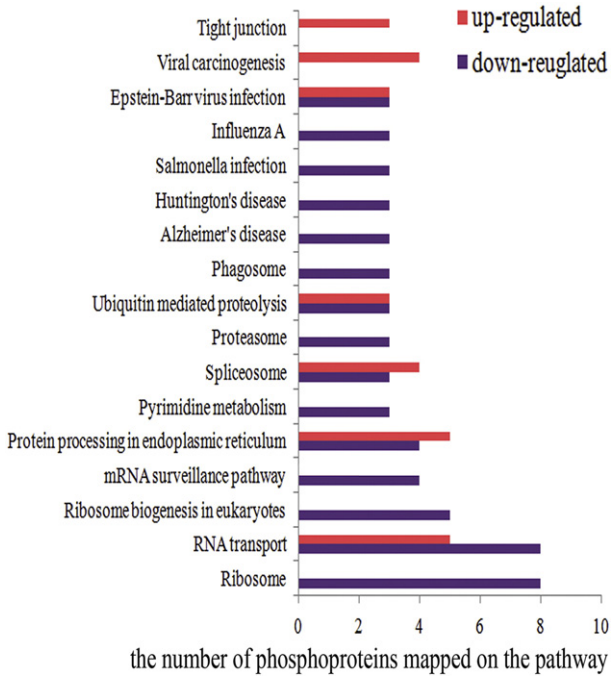

Fig. 5. KEGG pathways mapped by the differentially phosphorylated proteins. The lower panel shows the number of proteins mapping to the pathways. The light red pillar represents the increased phosphoproteins, and the purple pillar represents decreased phosphoproteins.

protein synthesis. In the biological process, a total of 10 GO terms were enriched by down-regulated phosphoproteins. The enriched translation, gene expression process and several biosynthetic processes indicate that protein synthesis and material accumulation are more active in the IC strain.

There were 7 pathways were enriched by up-regulated phosphoproteins, however 15 pathways were enriched by the down-regulated phosphoproteins (Fig. 5). Of these 15 pathways, most of them were related to protein synthesis. For instance, the RNA transport pathway enriched by most phosphoproteins in low abundance level suggest the function of this pathway may be hindered. Synthesizing large quantities of fibroin proteins requires active tRNA transport, thereby ensuring the efficiency of fibroin synthesis of the IC strain. The numerous down-regulated phosphoproteins mapped to ribosome pathway suggest that the translational machinery might be functionally reduced in the IN strain. Consequently, the synthetic quantity of fibroin and other proteins may be reduced, thus resulting in disintegration of PSG with no proteins filled. In addition, ribosome biogenesis in eukaryotes and mRNA surveillance pathway were specifically annotated by the down-regulated phosphoproteins. All these observations support a fact that the declined protein synthesis might be accounting for significantly reduced capacity in producing fibroin in the IN strain.

4. Conclusions

We reported the first phosphoproteome data of PSG of *B. mori*. Ser is preferentially phosphorylated, and acidic and proline-directed kinase classes may carry out the main phosphorylation events. The motif S-P-P is uniquely identified in the IC strain, and its kinase might be important for phosphorylation regulation of producing a large number of silk proteins. Phosphorylation may drive low silk production in the following four aspects. First, the decreased phosphorylation of several ribosomal proteins and regulatory factors may associate with the reduced protein synthesis. Second, the decreased phosphoproteins related to transport and secretion imply their roles in negative regulation of de novo protein synthesis. Third, the up-regulation of energy metabolism in IN indicates that energy turnover is likely related to the metabolism of substances other than silk proteins. Last but not least, the dephosphorylation of Fib-H may inhibit the formation of the silk structure by blocking silk protein secretion into the silk gland cavity. This reported data here gain a new understanding that the phosphorylation events implicate in regulating metabolism of silk synthesis.

Supplementary data to this article can be found online at http://dx.doi.org/10.1016/j.jprot.2016.08.007.

Conflict of interest

The authors declare that no conflict of interest exists in the submission of this manuscript, and manuscript is approved by all authors for publication.

Acknowledgment

This work was supported by the National Basic Research Program of China (No. 2012CB114601), China Postdoctoral Science Foundation (No. 518000-X91601) and the Projects of Zhejiang Provincial Science and Technology Plans (No. 2013C32048).

References

[1] L.D. Yonathan, P. Tony, D. Ivan, Post-translational modifications in signal integration, Nat. Struct. Mol. Biol. 17 (2010) 666–672.
[2] J.C. Alain, Protein phosphorylation in bacteria, Trends Biochem. Sci. 9 (1984) 400–403.
[3] B. Zhai, J. Villen, S.A. Beausoleil, J. Mintseis, S.P. Gyqi, Phosphoproteome analysis of *Drosophila melanogaster* embryos, J. Proteome Res. 7 (2008) 1675–1682.
[4] K.A. Resing, N.G. Ahn, Protein phosphorylation analysis byelectrospray ionization-mass spectrometry, in: W. DL (Ed.), Methods in Enzymology, Vol 5: Protein Phosphorylation Analysis by Eletrospray Mass Spectrometry: A Guide to Concept and Practice, Royal Society of Chemistry, New York, 2010.
[5] R. Aebersold, D.R. Goodlett, Mass spectrometry in proteomics, Chem. Rev. 101 (2001) 269–295.
[6] K. Mita, M. Kasahara, S. Sasaki, Y. Nagayasu, T. Yamada, H. Kanamori, N. Namiki, H. Yamashita, K. Yamamoto, M. Ajimura, M. Shimomura, Y. Nagamura, T. Sasaki, M. Kitagawa, Y. Yasukochi, K.K. Okuda, G. Ravikumar, L.T. Shin, H. Abe, T. Shimada, S. Morishita, The genome sequence of silkworm, *Bombyx mori*, DNA Res. 11 (2004) 27–35.
[7] F. Takei, F. Oyama, K. Kimura, A. Hyodo, S. Mizuno, K. Shimura, Reduced level of secretion and absence of subunitcombination for the fibroin synthesized by a mutant silkworm Nd(2), J Cell Biol. 99 (1984) 2005–2010.
[8] R.Z. Chang, Studies and utilization of isolines in soybeans.Soybean, Science 10 (1991) 64–68.
[9] J.Y. Li, H.J. Yang, T.Y. Lan, H. Wei, H.R. Zhang, M. Chen, Expression profiling and regulation of genes related to silkworm posterior silk gland development and fibroin synthesis, J. Proteome Res. 10 (2011) 3551–3564.
[10] S.H. Wang, Z.Y. You, L.P. Ye, J.Q. Che, Q.J. Qian, Y.H. Nanjo, S.S. Komatsu, B.X. Zhong, Quantitative proteomic and transcriptomic analyses of molecular mechanisms associated with low silk production in silkworm *Bombyx mori*, J. Proteome Res. 13 (2014) 735–751.
[11] Z.H. Zhou, H.J. Yang, M. Chen, C.F. Lou, Y.Z. Zhang, K.P. Chen, Y. Wang, M.L. Yu, F. Yu, Z.Y. Li, B.X. Zhong, Comparative proteomic analysis between the domesticated silkworm (*Bombyx mori*) reared on fresh mulberry leaves and on artificial diet, J. Proteome Res. 7 (2008) 5103–5111.
[12] S.H. Sui, J.L. Wang, B. Yang, L.N. Song, J.Y. Zhang, M. Chen, Phosphoproteome analysis of the human Chang liver cells using SCX and a complementary mass spectrometric strategy, Proteomics 8 (2008) 2024–2034.
[13] Y. Chen, W. Hoehenwarter, W. Weckwerth, Comparative analysis of phytohormone-responsivephosphoproteins in *Arabidopsis thaliana* using TiO_2-phosphopeptide enrichment and mass accuracyprecursor alignment, Plant J. 63 (2010) 1–17.
[14] J.E. Elias, S.P. Gygi, Target-decoy search strategy for increased confidence in large-scale protein identifications by mass spectrometry, Nat. Methods 4 (2007) 207–214.
[15] M.O. Collins, L. Yu, J.S. Choudhary, Analysis of protein phosphorylation on a proteome-scale, Proteomics 7 (2007) 2751–2768.
[16] J. Dai, L.S. Wang, Y.B. Wu, Q.H. Sheng, J.R. Wu, C.H. Shieh, R. Zeng, Fully automatic separation and identification of phosphopeptides by continuous pH-gradient anion exchange online coupled with reverse-phase liquid chromatography mass spectrometry, J. Proteome Res. 8 (2009) 133–141.
[17] D. Schwartz, S.P. Gygi, An iterative statistical approach to the identification of protein phosphorylation motifs from large-scale data sets, Nat. Biotechnol. 23 (2005) 1391–1398.
[18] J. Villen, S.A. Beausoleil, S.A. Gerber, S.P. Gygi, Large-scale phosphorylation analysis of mouse liver, Proc. Natl. Acad. Sci. U. S. A. 104 (2007) 1488–1493.
[19] E.A. Kuenzel, Krebs EG.A synthetic substrate specific for casein kinase II, Proc. Natl. Acad. Sci. U. S. A. 82 (1985) 737–741.

[20] E.A. Kuenzel, J.A. Mulligan, J. Sommercorn, E.G. Krebs, Substrate specificity determinants for casein kinase II as deducedfrom studies with synthetic peptides, J. Biol. Chem. 262 (1987) 9136–9140.
[21] G.H. Huang, X.G. Liu, N.C. Liang, Research progress of protein kinases CK2, Chem. Life 23 (2003) 169–171.
[22] D. Schwartz, S.P. Gygi, An iterative statistical approach to the identification of protein phosphorylation motifs from large-scale data sets, Nat. Biotechnol. 23 (2005) 1391–1398.
[23] Y.P. Qi, P. Fan, Y. Hao, B. Han, Y. Fang, M. Feng, Z.Y. Cui, J.K. Li, Phosphoproteomic analysis of protein phosphorylation networks in the hypopharyngeal gland of honeybee workers (*Apismelliferaligustica*), J. Proteome Res. 14 (2015) 4647–4661.
[24] M.D. Graauw, P. Hensbergen, B.V.D. Water, Phospho-proteomic analysis of cellular signaling, Electrophoresis 27 (2006) 2676–2686.
[25] M.K. Homma, I. Wada, T. Suzuki, J. Yamaki, K. EG, H. Yoshimi, CK2 phosphorylation of eukaryotic translation initiation factor 5 potentiates cell cycle progression, PNAS 102 (2005) 15688–15693.
[26] G.T. Sheu, J.A. Traugh, A structural model for elongation factor 1 (EF-1) and phosphrylation by protein kinase CKII, Mol. Cell. Biochem. 191 (1999) 181–186.
[27] E. Chevet, J. Smirle, P.H. Cameron, D.Y. Thomas, J.J.M. Bergeron, Calnexin phosphorylation: linking cytoplasmic signaling to endoplasmic reticulum luminal functions, Semin. Cell Dev. Biol. 21 (2010) 486–490.
[28] E. Chevet, H.N. Wong, D. Gerber, C. Cochet, A. Fazel, P.H. Cameron, J.N. Gushue, D.Y. Thomas, J.J.M. Bergeron, Phosphorylation by CK2 and MAPK enhances calnexin association with ribosomes, EMBO J. 18 (1999) 3655–3666.
[29] N.C. Price, L. Stevens, Fundamentals of Enzymology: The Cell and Molecular Biology of Catalytic Protein, Oxford University Press, New York, 2002.
[30] K. Mikulik, P. Suchan, J. Bobek, Changes in ribosome function induced by protein kinase associated with ribosomes of *Streptomyces collinus* producing kirromycin, Biochem. Biophys. Res. Commun. 289 (2001) 434–443.
[31] K. Mikulik, I. Janda, Protein kinase associated with ribosomes phosphorylates ribosomal proteins of *Streptomyces collinus*, Biochem. Biophys. Res. Commun. 238 (1997) 370–376.
[32] M. Remacha, A. Jimenezdiaz, C. Santo, E. Briones, R. Zambrano, G.M.A. Rodriguez, E. Guarinos, J.P. Ballesta, Proteins P1, P2, and P0, components of the eukaryotic ribosome stalk. New structural and functional aspects, Biochem. Cell Biol. 73 (1995) 959–968.
[33] E.J. Cho, M.S. Kobor, M. Kim, J. Greenblatt, S. Buratowski, Oppsing effects of Ctk1 kinase and Fcp1 phosphatase at Ser 2 of the RNA polymerase II C-terminal domain, Genes Dev. 15 (2001) 3319–3329.
[34] G. Song, G. Ouyang, S. Bao, The activation of Akt/PKB signaling pathway and cell survival, J. Cell. Mol. Med. 9 (2005) 59–71.
[35] A. Palamarchuk, A. Efanov, V. Maximov, R.I. Aqeilan, C.M. Croce, Y. Pekarsky, Aktphosphorylates and regulates Pdcd4 tumor suppressor protein, Cancer Res. 65 (2005) 11282–11286.
[36] K. Hojlund, Z. Yi, N. Lefort, P. Langlais, B. Bowen, K. Levin, H.B. Bielsen, L.J. Mandarino, Human ATP synthase beta is phosphorylated at multiple sites and shows abnormal phosphorylation at specific sites in insulin-resistant muscle, Diabetologia 53 (2010) 541–551.
[37] W.Q. Chen, H. Priewalder, J.P. John, G. Lubec, Silk cocoon of *Bombyx mori*: proteins and posttranslational modifications-heavy phosphorylation and evidence for lysine-mediated cross links, Proteomics 10 (2010) 369–379.
[38] H. Ueda, A. Hyodo, F. Takei, H. Sasaki, Y. Ohshima, K. Shimura, Sequence polymorphisms in the 5′-upstream region of the fibroin H-chain gene in the silkworm, *Bombyx mori*, Gene 28 (1984) 241–248.
[39] I. Amm, T. Sommer, D.H. Wolf, Protein quality control and elimination of protein waste: the role of the ubiquitin-proteasome system, Biochim. Biophys. Acta, Mol. Cell Res. 2014 (1843) 182–196.
[40] A. Reuner, S. Hengherr, B. Mali, F. Förster, D. Arndt, R. Reinhardt, T. Dandekar, M. Frohme, F. Brümmer, R.O. Schill, Stress response in tardigrades: differential gene expression of molecular chaperones, Cell Stress Chaperones 15 (2010) 423–430.
[41] M. Mollapour, S. Tsutsumi, L. Neckers, Hsp90 phosphorylation, Wee 1, and the cell cycle, Cell Cycle 9 (2010) 2310–2316.
[42] C. Liu, Y.L. Chen, F.Y. Dai, Y. Han, L.W. Wei, P.Y. Liu, J.B. Ren, Q.Y. Xia, Morphological observation of silk gland development in Nd mutant of silkworm, Newsl. Sericult. Sci. 1 (2010) 12–18.
[43] M. Koreishi, S. Yu, M. Oda, Y. Honjo, A. Satoh, CK2 phosphorylates Sec31 and regulates ER-to-Golgi trafficking, PLoS One 8 (2013) 1–9.